Journal of the Ceramic Society of Japan 130 [7] 464-470 2022
DOI http://doi.org/10.2109/jcersj2.21178

JCS-Japan

FULL PAPER

Preparation and characterization of epitaxially grown yttria-stabilized zirconia thin films on porous silicon substrates for solid oxide fuel cell applications

Haruki Zayasu[1], Takahiko Kawaguchi[1], Hiroki Nakane[1], Nobuyoshi Koshida[2], Kazuo Shinozaki[3,4], Hisao Suzuki[1,3,5], Naonori Sakamoto[1,3] and Naoki Wakiya[1,3,5,†]

[1] Graduate School of Integrated Science and Technology, Department of Engineering, Shizuoka University, 3–5–1 Johoku, Naka-ku, Hamamatsu 432–8561, Japan
[2] Graduate School of Engineering, Tokyo University of Agriculture and Technology, 2–24–16 Naka-cho, Koganei, Tokyo 184–8588, Japan
[3] Research Institute of Electronics, Shizuoka University, 3–5–1 Johoku, Naka-ku, Hamamatsu 432–8561, Japan
[4] School of Materials and Chemical Technology, Tokyo Institute of Technology, 2–12–1 O-okayama, Meguro-ku, Tokyo 152–8550, Japan
[5] Graduate School of Science and Technology, Shizuoka University, 3–5–1 Johoku, Naka-ku, Hamamatsu 432–8561, Japan

Epitaxial growth of yttria-stabilized zirconia (YSZ) thin film on through-hole-type porous silicon [tht-PSi(001)] with vertical pores penetrating from the surface to the back side of the Si(001) substrate was achieved. The in-plane and out-of-plane lattice parameters of YSZ thin film deposited on the tht-PSi(001) were, respectively 0.5167 and 0.5124 nm. Therefore, 0.54 % tensile strain was applied to the YSZ thin film. Also for this work, an all epitaxially grown thin film of YSZ/$La_{0.7}Sr_{0.3}MnO_3$(LSMO)/CeO_2/YSZ/Si(001) was prepared. The out-of-plane lattice parameter of YSZ was 0.5145 nm. Therefore, the YSZ thin film of YSZ/LSMO/CeO_2/YSZ/Si(001) is almost relaxed, with a small amount of tensile strain (0.12 %). In-plane and out-of-plane electrical properties were measured respectively for YSZ/tht-PSi(001) and YSZ/LSMO/CeO_2/YSZ/Si(001) thin films. Results show that ionic conduction was confirmed at 400 °C through constant electric conductivity against the change of oxygen partial pressure (pO_2). Enhanced ionic conduction was observed for epitaxial YSZ/tht-PSi(001) thin films measured along the in-plane direction. Such enhanced ionic conduction was not observed for epitaxial YSZ/LSMO/CeO_2/YSZ/Si(001) thin films measured along the out-of-plane direction. These findings suggest that enhanced ionic conduction is correlated with tensile strain in YSZ thin films.
©2022 The Ceramic Society of Japan. All rights reserved.

Key-words : Dynamic aurora PLD, Epitaxial, Ionic conduction, Strain, Through-hole-type porous silicon (tht-PSi), Yttrium stabilized zirconia (YSZ)

[Received December 25, 2021; Accepted March 14, 2022]

1. Introduction

Fuel cell systems are among the cleanest and the most environmentally friendly energy conversion technologies, offering numerous benefits such as the ability to provide heat and power with efficiencies exceeding 70 %. Furthermore, solid oxide fuel cells (SOFCs) are superior because they combine high system efficiency with fuel flexibility. Conventional SOFCs based on yttria-stabilized zirconia (YSZ) are operated at temperatures as high as 750 °C. Because of this high-temperature operation, cost and thermal issues have come to present major challenges. To address these issues, one good solution is to lower the operating temperature.[1)–5)] In addition, fuel cells that operate at lower temperatures allow shorter start-up times and reduced thermal cycling. One method of lowering the operating temperature is to use a thinner electrolyte. Reducing the solid electrolyte layer thickness is thought to reduce the impedance of ionic conduction and thereby lower the operating temperature.[2)–5)] However, thinning also presents the difficulty that it requires a substrate, which is expected to interfere with the fuel gas supply. Therefore, in earlier thin-film SOFCs, the gas is supplied from the back side of the substrate. To supply the gas from the back side of substrate, etching to remove part of

† Corresponding author: N. Wakiya; E-mail: wakiya.naoki@shizuoka.ac.jp
‡ Preface for this article: DOI http://doi.org/10.2109/jcersj2.130.P7-1

©2022 The Ceramic Society of Japan

This is an Open Access article distributed under the terms of the Creative Commons Attribution License (https://creativecommons.org/licenses/by/4.0/), which permits unrestricted use, distribution, and reproduction in any medium, provided the original work is properly cited.

substrate has been conducted.[6] However, etching might damage the thin films. Furthermore, etching requires expensive apparatus such as reactive ion etching.

In this work, we propose preparation of a thin film electrolyte (YSZ) deposited on a through-hole-type porous silicon (tht-PSi). The tht-PSi has penetrating vertical pores from the surface of the Si substrate to the back side. Moreover, it is expected to have permeability for gases, which suggests that thin film SOFC can be realized without post deposition processing such as etching. In addition, because tht-PSi maintains the crystal structure of silicon, it will be possible to realize epitaxially grown YSZ thin films on the tht-PSi. Reportedly, the ionic conductivity of epitaxially grown YSZ thin films increased by about one order of magnitude compared to that of bulk YSZ.[7] Therefore, enhanced ionic conductivity is expected for epitaxial YSZ thin films deposited on tht-PSi. No report of the relevant literature describes preparation of epitaxial YSZ on tht-PSi.

For the thin film SOFC application, both bottom and top electrodes are necessary for the electrolyte. To realize epitaxial growth of electrolyte (YSZ) thin films, epitaxial growth of the bottom electrode is needed. In the SOFC application, $La_{0.7}Sr_{0.3}MnO_3$ (LSMO) is used widely as a bottom electrode because LSMO is stable up to elevated temperatures. Nevertheless, it is impossible to realize epitaxial LSMO directly on the Si(001) substrate. Introducing a CeO_2/YSZ double buffer layer is known to facilitate the epitaxial growth of perovskite-type oxides such as LSMO on Si(001).[8)–11] Numerous reports have described the epitaxial growth of perovskite type oxides (such as LSMO) on fluorite-type oxides (such as CeO_2/YSZ), but few reports have described the epitaxial growth of fluorite type oxide on perovskite-type oxides. Scigaj et al. and Zhao et al. respectively reported an epitaxial YSZ thin film on $SrTiO_3$(011) and a CeO_2 thin film on $SrTiO_3$(001).[12,13] For this work, preparation of all epitaxial YSZ/LSMO/CeO_2/YSZ thin films was tried on Si(001) and on tht-PSi(001). Here, the first YSZ layer is deposited as a buffer layer to realize direct epitaxial growth on Si(001) and tht-PSi(001). The CeO_2 layer is used to reduce lattice mismatch between YSZ and LSMO layers. The LSMO layer is used as a bottom electrode. The second YSZ layer is the electrolyte layer. This work has three objectives. The first objective is to clarify the possibility of realizing epitaxial growth of YSZ on tht-PSi(001). The second objective is to clarify the possibility of realizing all epitaxial YSZ/LSMO/CeO_2/YSZ thin films on Si(001) and tht-PSi(001). The third objective is clarification of the electrical properties of epitaxial YSZ thin film.

2. Experimental

Porous Si (PSi) was prepared by electrochemical anodization of Sb-doped polished n-type Si(001) wafers with resistivity of 0.008–0.02 Ω cm. After the wafers were placed into a laboratory-made Teflon holder, they were connected to the anode of a potentiostat/galvanostat (HAL3001A with attached 10 A booster unit; Hokuto Denko Corp., Japan). A Pt wire was connected to the potentiostat/galvanostat cathode. The electrolyte contains 46–48 % aqueous hydrogen fluoride (HF) and 99.5 % ethanol with a volume mixing ratio of 1:1 (27.3 wt % of HF). Anodization was done using the galvanostat mode of 50 mA/cm^2 for 1800 s. Furthermore, tht-PSi was prepared by electropolishing, which was conducted by the rapid increase of current density of anodization to peel off the porous layer [tht-PSi(001)]. The tht-PSi(001) thickness was 90 µm. The tht-PSi(001) morphology was observed using scanning electron microscopy (SEM, JSM-7001F; JEOL). Thin film deposition was conducted using dynamic aurora PLD with a Nd:YAG laser ($\lambda = 266$ nm) on Si(001) with native oxide and tht-PSi(001) substrates. Dynamic aurora PLD is a kind of PLD by which an electromagnet is installed in the vacuum chamber between a target and a substrate. Therefore, a magnetic field parallel to the direction from the target to the substrate can be applied during thin film deposition. Our earlier work revealed that application of a magnetic field during deposition brings about convergence of the PLD plume (plasma) to increase the deposition rate.[14,15] For this study, thin film deposition was conducted under a 40–100 mT magnetic field. Detailed deposition conditions are presented in **Table 1**. The surface crystal structure of thin film was observed using reflection high-energy electron diffraction (RHEED) after turning off the magnetic field. The crystal structure of the thin films deposited on Si and tht-PSi was also examined using an X-ray diffractometer (MRD; Malvern Panalytical Ltd., UK). The thin film composition and thickness were analyzed using an X-ray fluorescence spectrometer (XRF) (Minipal; PANalytical B.V.) equipped with the FP Multi software module.

Electrical properties of YSZ thin film were evaluated using a potentiostat/galvanostat (VersaSTAT 4; Ametek Science Instruments, U.S.). From the results of AC impedance measurements, the electrical conductivities (σ) were calculated using the following equation.

$$\sigma = \frac{1}{R} \times \frac{L}{S} \tag{1}$$

Therein, R, L, and S respectively represent resistance, inter-electrode distance, and electrode area. Temperature dependence of electrical conductivity was measured at 200–450 °C in air. The oxygen partial pressure (pO_2) dependence of electrical conductivity was measured at 400 °C between 10^{-15} and 10^0 atm of pO_2. The pO_2 control was conducted using a PID-type oxygen partial pressure controller (SiOC-200S2; STLab Co. Ltd.). Detailed measurement conditions of electrical properties are presented in **Table 2**.

3. Results and discussion

Figures 1(a)–1(c) respectively depict SEM images of the surface, back side, and cross-section of tht-PSi(001) prepared using anodic oxidation. From Fig. 1(c), the porous layer [tht-PSi(001)] thickness was inferred as around 90 µm. Figure 1(d) portrays an enlarged image of

Table 1. Deposition conditions of (a) YSZ and (b) YSZ/LSMO/CeO_2/YSZ thin film

(a)

Laser	Nd:YAG laser ($\lambda = 266$ nm)
Repetition rate/Hz	10
Fluence J/cm^2	2.0
Substrate	tht-PSi(001) (90 µmt)
Target	YSZ (Y_2O_3 8 mol %)
Oxygen pressure/Pa	7.33×10^{-2}
Substrate temperature/°C	800
Magnetic field/mT	100

(b)

Laser	Nd:YAG laser ($\lambda = 266$ nm)			
Repetition rate/Hz	10			
Fluence J/cm^2	2.0			
Substrate	Si(001) and tht-PSi(001) (90 µmt)			
Target	YSZ (Y_2O_3 8 mol %)	CeO_2	$La_{0.7}Sr_{0.3}MnO_3$	YSZ (Y_2O_3 8 mol %)
Oxygen pressure/Pa	7.33×10^{-2}	7.33×10^{-2}	1.33×10^{-2}	1.33×10^{-2}
Substrate temperature/°C	800	800	750	800
Magnetic field/mT		40		100

Table 2. Measurement conditions of electrical properties

Laser	In-plane measurement	Out-plane measurement
Temperature/°C	200–400	300–450
Start frequency/Hz	10^6	
End frequency/Hz	1	
Amplitude/mV	1000	10
Applied voltage/V	1	0.01

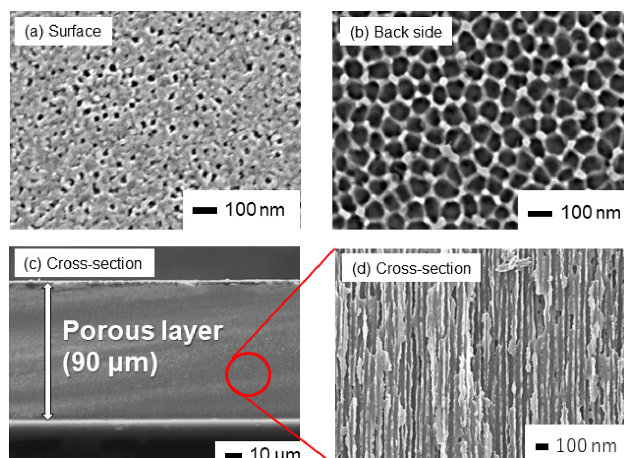

Fig. 1. SEM images of (a) surface, (b) back surface, (c) cross-section, and (d) enlarged image of the cross-section of tht-PSi(001).

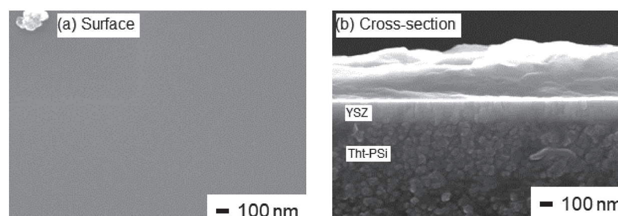

Fig. 2. SEM images of (a) surface and (b) cross-section of YSZ thin film deposited on tht-PSi(001).

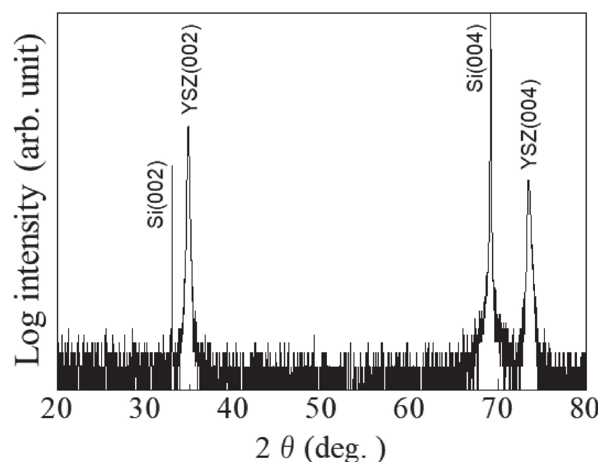

Fig. 3. XRD patterns of YSZ thin film deposited on tht-PSi(001).

the cross-section. These figures show that the tht-PSi(001) comprises vertical straight pores having 10 nm average pore diameter. The fraction of the surface pore analyzed using ImageJ software[16] was 12 %. Because the gas molecule size is on the order of 0.3 nm, it is considered that tht-PSi(001) can have gas permeation from the surface to the back side. **Figures 2**(a) and 2(b) portray SEM images of the surface and cross section of YSZ thin film deposited on the tht-PSi(001). These figures indicate that YSZ thin film has smooth morphology and that it is dense on the tht-PSi(001). The YSZ thin film thickness was 160 nm.

Figure 3 shows XRD patterns of YSZ thin film on tht-PSi(001) substrate. This figure shows that the YSZ thin film has (001) orientation. **Figures 4**(a) and 4(b) show (111) and (110) pole figures of YSZ thin film deposited on tht-PSi(001) substrate, measured respectively at $2\theta =$ 30.11 and 50.18°. The fact that only four poles are observed in both (111) and (110) pole figures suggests that the YSZ thin film is grown epitaxially on tht-PSi(001). The epitaxial growth of YSZ thin film deposited on tht-

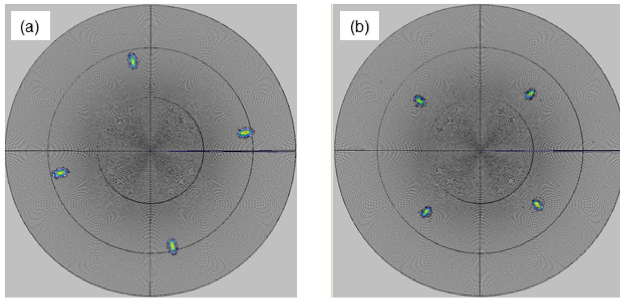

Fig. 4. (a) (111) and (b) (110) pole figures of YSZ thin film deposited on tht-PSi(001).

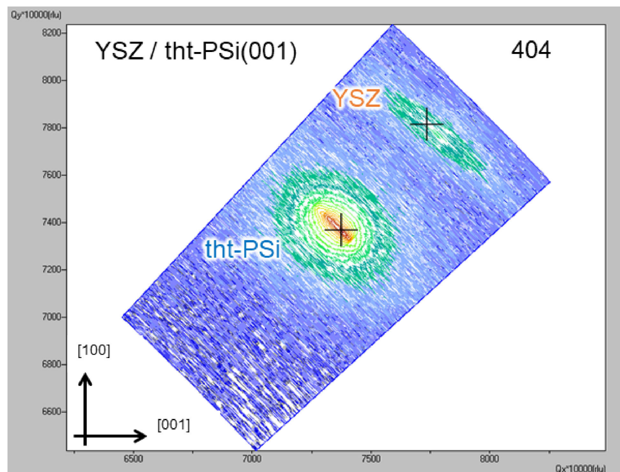

Fig. 5. Reciprocal space map of YSZ/tht-PSi(001) thin film around YSZ(404).

PSi(001) was also confirmed by a reciprocal space map measured at around YSZ(404) as presented in **Fig. 5**. From this figure, the in-plane and out-of-plane lattice parameters of YSZ thin films were calculated respectively as 0.5167 and 0.5124 nm. Because the lattice parameter of YSZ bulk is $a = 0.5139$ nm, the result presented in Fig. 5 means that tensile strain of 0.54 % is applied along in-plane direction for YSZ/tht-PSi(001) thin film.

Figure 6 shows XRD patterns of (a) YSZ, (b) CeO_2/YSZ, (c) LSMO/CeO_2/YSZ, and (d) YSZ/LSMO/CeO_2/YSZ thin film deposited on Si(001). This figure indicates that all layers have *c*-axis orientation. The thicknesses of the first YSZ, CeO_2, LSMO, and second YSZ layers measured using XRF were, respectively, 10, 8.6, 90, and 300 nm. **Figure 7** portrays RHEED images of (a) YSZ, (b) CeO_2/YSZ, (c) LSMO/CeO_2/YSZ, and (d) YSZ/LSMO/CeO_2/YSZ thin films deposited on Si(001) recorded along azimuth Si[110]. All RHEED images show a streak pattern that indicates epitaxial growth.[17] It is noteworthy that the RHEED patterns of Figs. 7(a) and 7(d) are the same. Therefore, the YSZ layer deposited on the LSMO layer is grown epitaxially, having the same in-plane orientation as the first deposited YSZ layer. **Figure 8** depicts XRD patterns of YSZ/LSMO/CeO_2/YSZ thin film deposited on (a) tht-PSi(001) and (b) Si(001). Compared with the XRD pattern deposited on Si(001), the film deposited on tht-PSi(001) has low crystallinity. Especially, the peak of

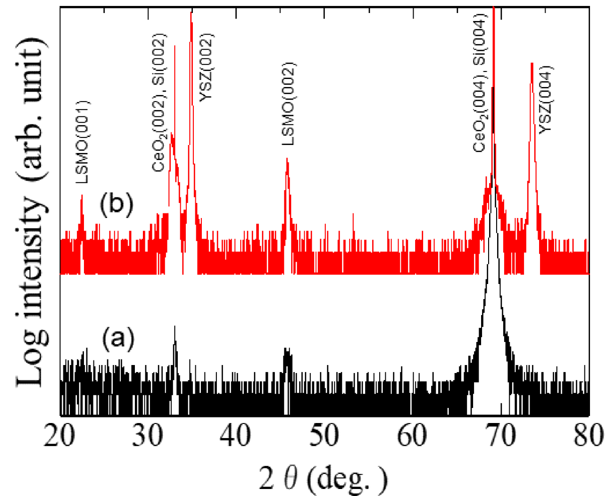

Fig. 6. XRD patterns of (a) YSZ, (b) CeO_2/YSZ, (c) LSMO/CeO_2/YSZ, and (d) YSZ/LSMO/CeO_2/YSZ thin film deposited on Si(001).

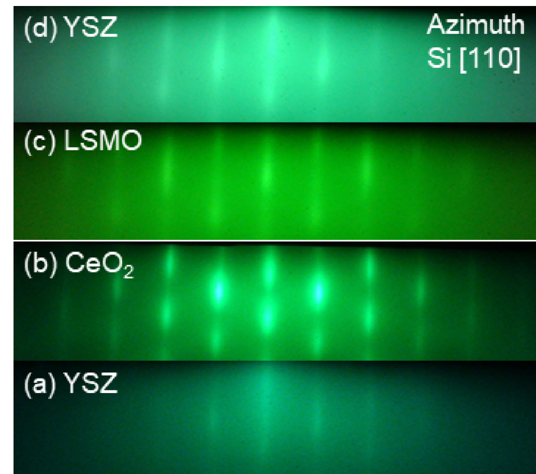

Fig. 7. RHEED images of (a) YSZ, (b) CeO_2/YSZ, (c) LSMO/CeO_2/YSZ, and (d) YSZ/LSMO/CeO_2/YSZ thin film deposited on Si(001) recorded along azimuth Si[110].

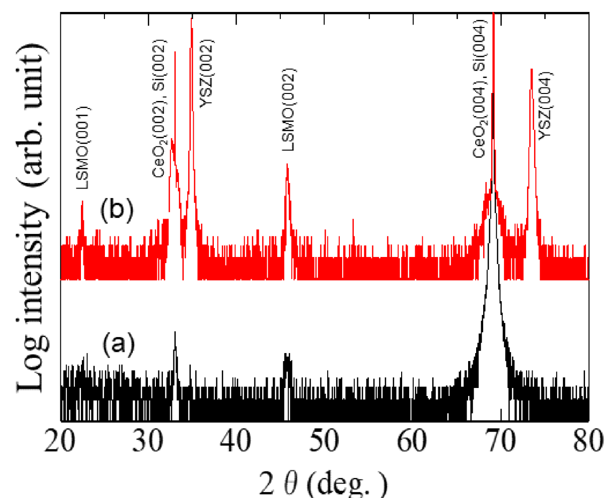

Fig. 8. XRD patterns of YSZ/LSMO/CeO_2/YSZ thin film deposited on (a) tht-PSi(001) and (b) Si(001).

the YSZ layer is not observed for the film deposited on tht-PSi(001). **Figure 9** portrays RHEED images of (a) YSZ/LSMO/CeO_2/YSZ thin films deposited on (a) tht-PSi(001) and (b) Si(001), subsequently recorded along the azimuth Si[110]. No streak is observed for YSZ/LSMO/CeO_2/YSZ thin film deposited on tht-PSi(001). The results presented in Figs. 8(a) and 9(a) indicate that the second YSZ layer deposited on LSMO layer has very low crystallinity. As presented in Figs. 4 and 5, the first YSZ layer is epitaxially grown on tht-PSi(001). However, the crystallinity was much lower than the film deposited on Si(001). The low crystallinity succeeded to the upper layers of CeO_2, LSMO and second YSZ. The low crystallinity of the second YSZ layer was regarded as derived by cumulative low crystallinity.

For this work, in-plane and out-of-plane electrical properties were measured respectively for YSZ/tht-PSi(001) and YSZ/LSMO/CeO_2/YSZ/Si(001) thin films. For the in-plane electrical property measurement, 6 mm × 1 mm rectangular Pt electrodes were fabricated through a metal mask. On the surface of the rectangular Pt electrode, Pt wires (0.1 mmϕ) were attached using a small amount of Ag paste. Then the wires were connected to the measurement system probe, as presented in **Fig. 10**(a). For out-of-plane electrical property measurements, 0.1 mmϕ circular Pt top electrodes were fabricated through a metal mask. On the surfaces of the Pt top electrode and the LSMO bottom electrode, Pt wires (0.1 mmϕ) were attached using small amount of Ag paste. Then the wires were connected to the measurement system probe, as shown in Fig. 9(b). **Figure 11**(a) shows the temperature dependence of Nyquist plots of the YSZ/tht-PSi(001) thin film measured for the in-plane direction. Figure 11(b) shows that of YSZ/LSMO/CeO_2/YSZ/Si(001) thin film measured along the out-of-plane direction. The thin film resistance was calculated based on the radii of semicircles. **Figure 12** shows the change of electric conductivity with pO_2. Measurements were conducted at a constant temperature of 400 °C with gas flowing in for a sufficient time (more than 10 min) to make the measurement atmosphere a specific oxygen atmosphere. This figure shows that the electrical conductivity is unchanged with pO_2 between 10^{-15} and 10^0 atm. Reportedly, if the carrier is electron, the electric conductance changes with pO_2.[18)–21)] The fact that the electrical conductivity of YSZ/tht-PSi(001) film is unchanged with pO_2 indicates that this

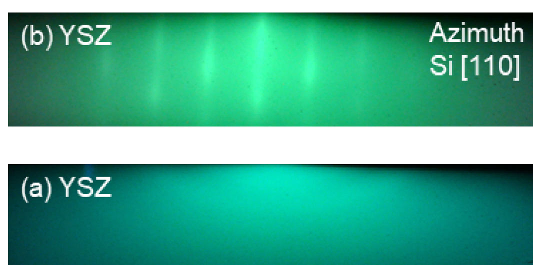

Fig. 9. RHEED images of (a) YSZ/LSMO/CeO_2/YSZ thin film deposited on (a) tht-PSi(001) and (b) Si(001) recorded along azimuth Si[110].

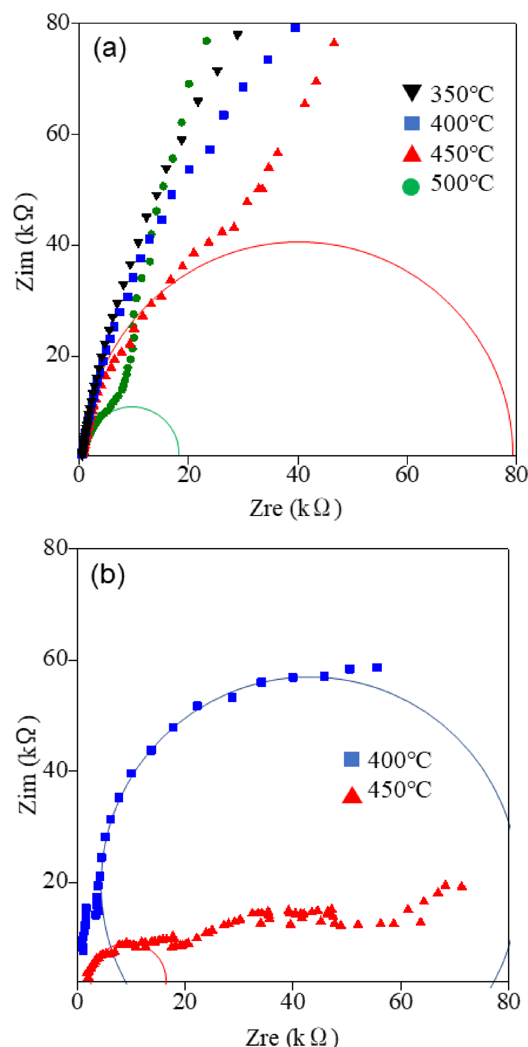

Fig. 11. Nyquist plots of (a) YSZ/tht-PSi(001) thin film (in-plane) and (b) YSZ/LSMO/CeO_2/YSZ/Si(001) thin film (out-of-plane).

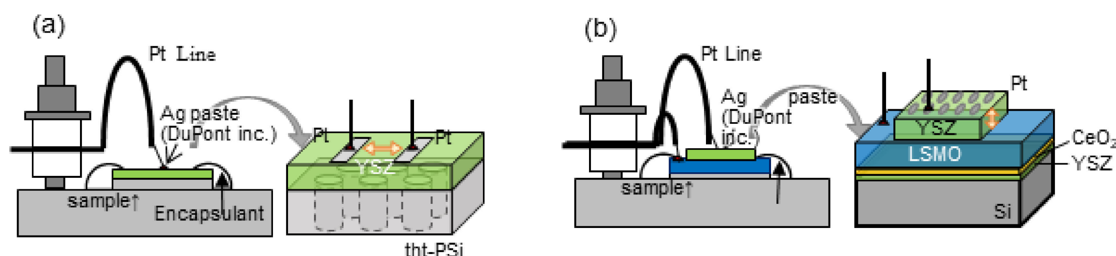

Fig. 10. Schematic drawing of electrical property measurement in (a) in-plane and (b) out-of-plane directions.

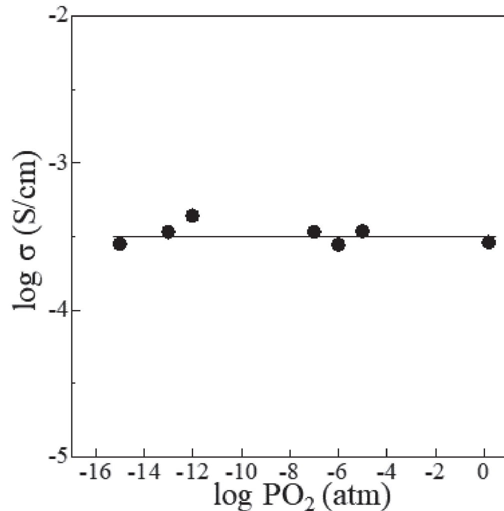

Fig. 12. Change of electrical conductivity of YSZ/tht-PSi(001) thin film (in-plane) with oxygen partial pressure measured at 400 °C.

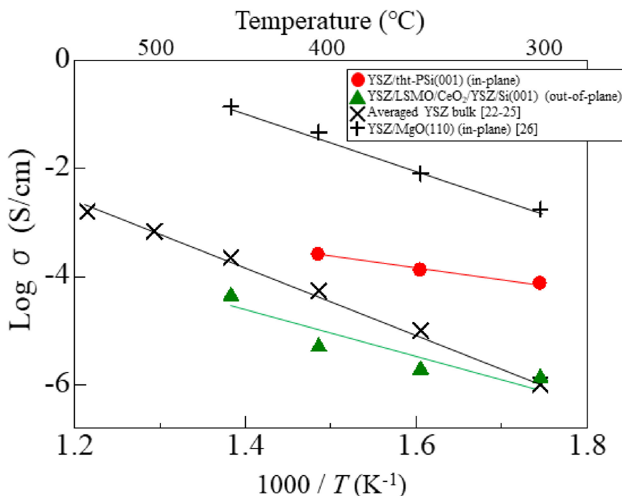

Fig. 13. Arrhenius plots of YSZ/tht-PSi(001)(in-plane) and YSZ/LSMO/CeO_2/YSZ/Si(001)(out-of-plane) thin films. Data of YSZ bulk taken by averaging reported data[22)–25)] and YSZ/MgO(110)(in-plane) thin film[26)] are shown for comparison.

film is ionic conduction. **Figure 13** shows Arrhenius plots of YSZ/tht-PSi(001)(in-plane) and YSZ/LSMO/CeO_2/YSZ/Si(001)(out-of-plane) thin films. Data of YSZ bulk taken by averaging reported data[22)–25)] and YSZ/MgO(001)(in-plane) thin film[26)] are also shown for comparison. These findings clarified that in-plane ionic conductivity of YSZ thin film deposited on tht-PSi(001) is higher than that of the bulk YSZ. This increase of ionic conductivity is regarded as brought about by 0.54 % of tensile strain described for Fig. 5. Similar enhancement of the in-plane ionic conductivity because of tensile strain is reported for YSZ thin film deposited on MgO(110) and (111) single crystals.[26)] In Fig. 13, data of YSZ/MgO(110) reported by Sillassen et al.[26)] are also shown for comparison. Results clarified that the out-of-plane ionic conductivity of the YSZ thin film deposited on LSMO/CeO_2/YSZ/Si(001) is almost equal to that of the YSZ bulk. The out-of-plane lattice parameter of YSZ in YSZ/LSMO/CeO_2/YSZ/Si(001) thin film was 0.5145 nm. This value is slightly larger than that of YSZ bulk (0.5139 nm). Therefore, the tensile strain along the out-of-plane direction was calculated as 0.12 %. Because this value is much smaller than the tensile strain of YSZ/tht-PSi(001) thin film, the YSZ layer in YSZ/LSMO/CeO_2/YSZ/Si(001) is almost relaxed. This relaxation is inferred as the reason why enhanced ionic conductivity was observed for the in-plane direction of the YSZ/tht-PSi(001) thin film, and not observed for the out-of-plane direction of the YSZ/LSMO/CeO_2/YSZ/Si(001) thin film. Therefore, these results suggest that enhanced ionic conduction is correlated to tensile strain in YSZ thin films deposited on tht-PSi(001).

4. Conclusions

In this work, we realized epitaxial growth of YSZ thin film on tht-PSi(001) using dynamic aurora PLD. The in-plane and out-of-plane lattice parameters of YSZ thin films measured using reciprocal space map measurement were, respectively 0.5167 and 0.5124 nm. Therefore, 0.54 % of tensile strain is applied for the YSZ thin film.

Preparation of all epitaxial YSZ/LSMO/CeO_2/YSZ thin film succeeded on the Si(001) substrate. The out-of-plane lattice parameter of YSZ was 0.5145 nm. Therefore, the YSZ thin film of YSZ/LSMO/CeO_2/YSZ/Si(001) is almost relaxed with small amount of tensile strain (0.12 %). Although we tried to prepare epitaxial YSZ/LSMO/CeO_2/YSZ thin film on the tht-PSi(001), it was difficult to confirm epitaxial growth because of the low crystallinity.

In-plane and out-of-plane electrical properties were measured respectively for YSZ/tht-PSi(001) and YSZ/LSMO/CeO_2/YSZ/Si(001) thin films. Results show that ionic conduction was confirmed at 400 °C through the change of electric conductivity with oxygen partial pressure (pO_2). Enhanced ionic conduction was observed for epitaxial YSZ/tht-PSi(001) thin films measured along in-plane direction. Such enhanced ionic conduction was not observed for epitaxial YSZ/LSMO/CeO_2/YSZ/Si(001) thin films along the out-of-plane direction. The findings suggest that enhanced ionic conduction is correlated to tensile strain in YSZ thin film.

Acknowledgments Part of this work was supported by a Grant-in-Aid for Scientific Research from the Ministry of Education, Culture, Sports, Science and Technology (No. 18H01705). Part of this work was conducted under the Cooperative Research Project Program of Research Institute of Electronics, Shizuoka University. Part of this research was also supported by the Collaborative Research Project of Laboratory for Materials and Structures, Institute of Innovative Research, Tokyo Institute of Technology.

References

1) E. Fabbri, L. Bi, D. Pergolesi and E. Traversa, *Adv. Mater.*, 24, 195–208 (2012).

2) Z. P. Shao and M. H. Sossina, *Nature*, 431, 170–173 (2004).
3) R. Doshi, V. L. Richards and J. D. Carter, *J. Electrochem. Soc.*, 146, 1273–1278 (1999).
4) A. Maheshwari and H. D. Wiemho, *Acta Mater.*, 103, 361–369 (2016).
5) N. Jaiswal, D. Kumar, S. Upadhyay and O. Parkash, *Ceram. Int.*, 7, 9004–9010 (2016).
6) H. Huang, *J. Electrochem. Soc.*, 154, B20–B24 (2007).
7) C. Korte, J. Keppner, A. Peters, N. Schichtel, H. Aydin and J. Janek, *Phys. Chem. Chem. Phys.*, 16, 24575–24591 (2014).
8) C. H. Chen, A. Saiki, N. Wakiya, K. Shinozaki and N. Mizutani, *J. Vac. Sci. Technol. A*, 20, 1749–1754 (2002).
9) S. Sawamura, N. Wakiya, N. Sakamoto, K. Shinozaki and H. Suzuki, *Jpn. J. Appl. Phys.*, 47, 7603–7606 (2008).
10) J. H. Kim, S. I. Khartsev and A. M. Grishin, *Appl. Phys. Lett.*, 82, 4295–4297 (2003).
11) N. Wakiya, T. Azuma, K. Shinozaki and N. Mizutani, *Thin Solid Films*, 410, 114–120 (2002).
12) M. Scigaj, N. Dix, M. Cabero, A. Rivera-Calzada, J. Santamaria, J. Fontcuberta, G. Herranz and F. Sánchez, *Appl. Phys. Lett.*, 104, 251602 (2014).
13) P. Zhao, A. Ito and T. Goto, *Surf. Coat. Tech.*, 235, 273–276 (2013).
14) N. Wakiya, N. Sakamoto, S. Koda, W. Kumasaka, N. Debnath, T. Kawaguchi, T. Kiguchi, K. Shinozaki and H. Suzuki, *NPG Asia Mater.*, 8, e279 (2016).
15) N. Wakiya, T. Kawaguchi, N. Sakamoto, H. Das, K. Shinozaki and H. Suzuki, *J. Ceram. Soc. Jpn.*, 125, 856–865 (2017).
16) C. A. Schneider, W. S. Rasband and K. W. Eliceiri, *Nat. Methods*, 9, 671–675 (2012).
17) Y. Suzuki, *Mater. Jpn.*, 35, 53–59 (1996) [in Japanese].
18) A. Cavallaro, M. Burriel, J. Roqueta, A. Apostolidis, A. Bernardi, A. Tarancón, R. Srinivasan, S. N. Cook, H. L. Fraser, J. A. Kilner, D. W. McComb and J. Santiso, *Solid State Ionics*, 181, 592–601 (2010).
19) X. Guo, *Science*, 324, 465 (2009).
20) K. Sasaki, J. Claus and J. Maier, *Solid State Ionics*, 121, 51–60 (1999).
21) Z. Zhang, W. Sigle, R. A. De Souza, W. Kurtz, J. Maier and M. Rühle, *Acta Mater.*, 53, 5007–5015 (2005).
22) J. H. Joo and G. M. Choi, *Solid State Ionics*, 177, 1053–1057 (2006).
23) T. Ishihara, H. Eto, H. Zhong and H. Matsumoto, *J. Appl. Electrochem.*, 77, 115–122 (2009).
24) W. Shen and J. L. Hertz, *Chem. Mater.*, 3, 2378–2386 (2015).
25) J. Jiang, X. Hu, W. Shen, C. Ni and J. L. Hertz, *Appl. Phys. Lett.*, 102, 143901 (2013).
26) M. Sillassen, P. Eklund, N. Pryds, E. Johnson, U. Helmersson and J. Bøttiger, *Adv. Funct. Mater.*, 20, 2071–2076 (2010).